


## *Ypt4* and *lvs1* regulate vacuolar size and function in *Schizosaccharomyces pombe*

Addison Rains<sup>†</sup>, Yorisha Bryant<sup>†</sup>, Kaitlyn A. Dorsett<sup>†</sup>, Austin Culver<sup>†</sup>, Jamal Egbaria, Austin Williams, Matt Barnes, Raeann Lamere, Austin R. Rossi, Stephanie C. Waldrep, Caroline Wilder, Elliot Kliossis, and Melanie L. Styers 

Department of Biology, Birmingham-Southern College, Birmingham, AL, USA

### ABSTRACT

The yeast vacuole plays key roles in cellular stress responses. Here, we show that deletion of *lvs1*, the fission yeast homolog of the Chediak-Higashi Syndrome *CHS1/LYST* gene, increases vacuolar size, similar to deletion of the Rab4 homolog *ypt4*. Overexpression of *lvs1*-YFP rescued vacuolar size in *ypt4*Δ cells, but *ypt4*-YFP did not rescue *lvs1*Δ, suggesting that *lvs1* may act downstream of *ypt4*. Vacuoles were capable of hypotonic shock-induced fusion and recovery in both *ypt4*Δ and *lvs1*Δ cells, although recovery may be slightly delayed in *ypt4*Δ. Endocytic and secretory trafficking were not affected, but *ypt4*Δ and *lvs1*Δ strains were sensitive to neutral pH and CaCl<sub>2</sub>, consistent with vacuolar dysfunction. In addition to changes in vacuolar size, deletion of *ypt4* also dramatically increased cell size, similar to *tor1* mutants. These results implicate *ypt4* and *lvs1* in maintenance of vacuolar size and suggest that *ypt4* may link vacuolar homeostasis to cell cycle progression.

### ARTICLE HISTORY

Received 5 April 2017  
Revised 18 May 2017  
Accepted 22 May 2017

### KEYWORDS

Chediak-Higashi Syndrome; fission yeast; *lvs1*; *LYST*; *rab4*; vacuole; *ypt4*

### Introduction

Vacuoles are important players in numerous cellular processes in yeast. They regulate storage of water, ions, and nutrients; recycle organelles and macromolecules in response to damage or nutrient deprivation; and play a key role in the osmotic shock and other stress responses through regulated fusion and fission events.<sup>1,2</sup> Despite these common functions, the fission yeast vacuole differs substantially in morphology compared with the budding yeast vacuole. *Schizosaccharomyces pombe* cells are characterized by numerous small vacuoles, much like human lysosomes, rather than the one or few large, central vacuoles observed in *Saccharomyces cerevisiae*.<sup>3</sup> Although the molecular machinery that drives vacuolar-protein sorting is largely conserved between the two types of yeast,<sup>3</sup> the identities of the molecular players that mediate differences in vacuolar structure between the two organisms are currently unknown. Elucidation of these poorly explored mechanisms in fission yeast could shed new light on evolutionarily conserved lysosomal biogenesis pathways in mammalian systems.

A large body of evidence has identified a set of conserved genes that regulate the biogenesis of lysosomes and lysosome-related organelles (LROs) in mammalian systems.<sup>4</sup> Many of these genes have been shown to be associated with clinical disorders characterized by hypopigmentation and platelet storage pool deficiency in mice and humans,<sup>5</sup> although the precise cellular functions of their protein products are unclear in some cases. One of the least characterized of these pigment dilution genes is *CHS1/LYST*, the causative gene in Chediak-Higashi Syndrome (CHS) type 1.<sup>6</sup> CHS patients are characterized by hypopigmentation, immune and coagulation defects, and

neurologic issues at the phenotypic level and enlarged, lysosomes and lysosome-related organelles at the cellular level.<sup>6,7</sup> The cellular function of *Lyst* is unclear; *Lyst* and its homologs, all of which are characterized by the presence of a conserved BEACH domain,<sup>8</sup> have been proposed to serve in multiple functions related to lysosomal biogenesis and homeostasis. They have been suggested to act as positive regulators of lysosomal fission,<sup>9</sup> negative regulators of lysosomal fusion,<sup>10</sup> as well as positive regulators of post-lysosome and LRO biogenesis and fusion with the cell surface.<sup>11-13</sup> Importantly, the end result in each of these scenarios is the hallmark enlargement of lysosomes, post-lysosomes, and LROs observed in CHS. In contrast to *LYST* homologs in other organisms, deletion of the budding yeast *LYST* homolog, *BPH1*, does not result in enlarged vacuoles and only causes a mild defect in sorting of vacuolar proteins, suggesting that the BEACH protein may serve a different function in budding yeast.<sup>14</sup> The role of the fission yeast homolog of *LYST*, *lvs1*, in control of vacuolar size and function has not previously been characterized. However, *lvs1p* is 22.16% identical to human *LYST*, while *Bph1p* is only 14.86% identical to human *LYST* and 29.46% identical to *lvs1p*, suggesting that fission yeast *lvs1p* could share more conservation of function with the human protein.<sup>15</sup>

In fission yeast, antagonistic control of vacuolar size by the *sty1* mitogen-activated protein kinase (MAPK) pathway and protein phosphatase 2C plays an important role in the response to environmental stresses, such as osmotic shock or starvation.<sup>16,17</sup> The *sty1* homolog *Hog1p* has also been implicated in the osmotic response in budding yeast.<sup>18</sup> Similarly, homologs of *Rab7* (*ypt7/ypt71/YPT7*) have been implicated in regulation

**CONTACT** Melanie L. Styers  [mstyers@bsc.edu](mailto:mstyers@bsc.edu)  Department of Biology, Birmingham-Southern College, Box 549022, Birmingham, AL 35254, USA.

<sup>†</sup>These authors contributed equally.

© 2017 Addison Rains, Yorisha Bryant, Kaitlyn A. Dorsett, Austin Culver, Jamal Egbaria, Austin Williams, Matt Barnes, Raeann Lamere, Austin R. Rossi, Stephanie C. Waldrep, Caroline Wilder, Elliot Kliossis, and Melanie L. Styers. Published with license by Taylor & Francis.

This is an Open Access article distributed under the terms of the Creative Commons Attribution-NonCommercial-NoDerivatives License (<http://creativecommons.org/licenses/by-nc-nd/4.0/>), which permits non-commercial re-use, distribution, and reproduction in any medium, provided the original work is properly cited, and is not altered, transformed, or built upon in any way.

of vacuole and vacuole-endosome fusion in both types of yeast,<sup>19,20</sup> suggesting some level of mechanistic conservation between the 2 species. However, considering the differences in vacuolar morphology between fission and budding yeast, species-specific mechanisms that contribute to vacuolar homeostasis must also exist. One potential player in a fission yeast-specific mechanism that regulates vacuolar size is the Rab *ypt4*. Deletion of *ypt4* has been shown to result in increased vacuolar size,<sup>17</sup> but *ypt4* has no clear ortholog in *S. cerevisiae* according to Pombase (www.pombase.org).

The goal of this exploratory study was to characterize the unique mechanisms that contribute to vacuolar homeostasis in fission yeast. We compared the phenotypes of cells lacking *ypt4* and *lvs1*, the fission yeast homolog of *LYST*. By assessing cell and vacuolar morphology, membrane trafficking, and vacuolar function in these cells, we show that *lvs1p* likely acts downstream of *ypt4p* in regulation of vacuolar size and also link *ypt4p* to control of cell size. Our results establish fission yeast as a novel model for CHS. Fission yeast lacking *lvs1* had enlarged vacuoles, consistent with the enlarged lysosomes and lysosomal organelles that are the hallmark of this disorder.

## Results

To characterize the molecular pathways that control vacuolar homeostasis in fission yeast, we explored the phenotypes of strains with deletion of *lvs1*, the fission yeast homolog of human *LYST*, or *ypt4*, a gene previously shown to be associated with changes in vacuole size in fission yeast.<sup>17</sup> To assess vacuolar morphology, wildtype (WT), *lvs1Δ*, and *ypt4Δ* cells were stained with the yeast vacuole membrane stain MDY-64<sup>21</sup>. Both *ypt4Δ* and *lvs1Δ* cells had larger vacuoles than WT cells, with *ypt4Δ* cells appearing to have the largest vacuoles of the 3 strains (Fig. 1A). To quantify these results, we measured the

pixel area of the largest vacuole in each cell for all 3 strains and calculated the distribution of cells with vacuoles falling within one of four size-based bins. Quantification confirmed that the *ypt4Δ* cells had the largest vacuoles, although both *lvs1Δ* and *ypt4Δ* cells had vacuoles that were significantly larger than that of the WT cells (Fig. 1B).

In addition to enlarged vacuoles, initial morphological observations of *ypt4Δ* cells suggested that they were larger than WT or *lvs1Δ* cells. A similar phenotype been observed in cells lacking TORC2 activity,<sup>2,22</sup> suggesting the potential for a link between *ypt4* and control of cell division. To quantitatively assess the phenotype, we measured the lengths and widths of WT, *ypt4Δ*, and *lvs1Δ* cells captured using a differential interference contrast (DIC) filter. Results from this analysis revealed that *ypt4Δ* cells (Fig. 2A, C), but not *lvs1Δ* cells (Fig. 2B, D) exhibited a significantly greater length, width, and length:width ratio than WT cells.

To better understand the relationship between *ypt4p* and *lvs1p*, we next assessed vacuolar size in WT, *ypt4Δ*, and *lvs1Δ* cells overexpressing *ypt4*-YFP or *lvs1*-YFP. To visualize the vacuoles, cells were stained with the lipophilic dye FM4-64, which transits the endocytic pathway to reach the vacuole.<sup>23</sup> Quantification of vacuolar size using Image J revealed that, similar to results with MDY-64 (Fig. 1), both *ypt4Δ* and *lvs1Δ* cells had significantly larger vacuoles than the WT strain, with *ypt4Δ* vacuoles being the largest (Fig. 3A). Initial rescue experiments using *ypt4p* tagged at the N-terminus (YFP-*ypt4p*) generated a non-functional protein that did not rescue the *ypt4Δ* deletion mutant. In contrast, overexpression of C-terminally-tagged *ypt4*-YFP rescued the vacuolar phenotype in *ypt4Δ* cells. However, overexpression of *ypt4*-YFP did not reduce vacuolar size in WT or *lvs1Δ* cells, actually resulting in a slight enlargement in vacuolar size. Overexpression of *lvs1*-YFP rescued vacuolar size to WT levels in *ypt4Δ* cells and reduced vacuole size to smaller than WT in both WT and *lvs1Δ* strains. Because overexpression of *lvs1p* rescued loss of *ypt4*, but the converse was not true, these data suggest that *lvs1p* may act downstream of *ypt4p* to drive vacuolar fission (Fig. 3A). However, it is important to note that the C-terminally tagged *ypt4*-YFP did not properly localize to membranes, instead localizing throughout the cytoplasm, consistent with inhibition of geranylgeranylation on the 2 adjacent C-terminal cysteines of *ypt4*,<sup>24,25</sup> complicating the interpretation of these results.

To further explore the functional roles of *ypt4* and *lvs1*, we characterized the response of *ypt4Δ* and *lvs1Δ* cells to hypertonic shock by exposing FM4-64-stained cells to dH<sub>2</sub>O for 90 minutes (Fig. 3B). Consistent with previous studies,<sup>17</sup> vacuoles in *ypt4Δ* cells underwent fusion to form larger vacuoles (compare Fig. 3A, C). Similarly, enlarged vacuoles in the *lvs1Δ* strain were also capable of fusing to create larger vacuoles (compare Fig. 3A, C). However, although WT and *lvs1Δ* cells subjected to 90 minutes of recovery in normal media returned to normal vacuole size, *ypt4Δ* cells still possessed enlarged vacuoles after 90 min, suggesting that passive fission may be partially impaired in these cells [compare Fig. 3A, C; 17].

*Ypt4p* shares 47% identity with human Rab4,<sup>15</sup> which has previously been implicated in endosomal trafficking.<sup>26</sup> Furthermore, membrane trafficking pathways have been implicated in control of vacuolar size in yeast.<sup>27,28</sup> Therefore, we next

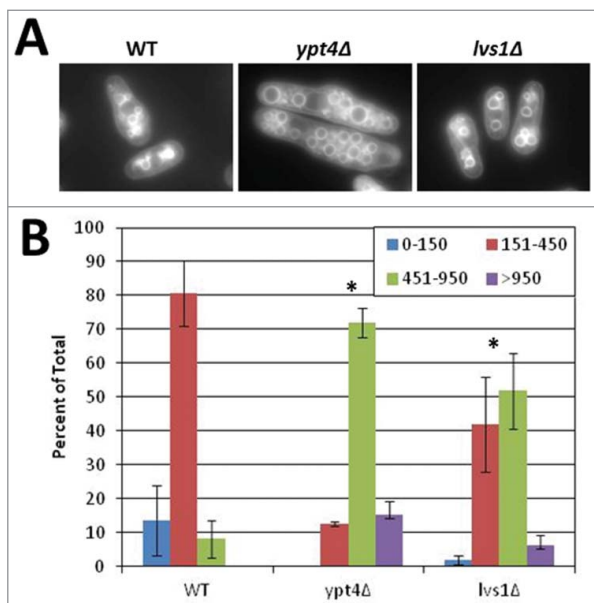


**Figure 1.** Deletion of *ypt4* or *lvs1* results in an increase in vacuole size. (A) Wildtype (WT), *ypt4Δ*, and *lvs1Δ* cells were stained with MDY-64, and vacuoles were visualized by fluorescence microscopy. (B) Quantification of A. The pixel area of the largest vacuole in each cell was measured using ImageJ software. The percentage of cells containing vacuoles of the indicated pixel areas were calculated for each strain. Data are presented as the mean  $\pm$  SEM. \* $p < 0.001$  vs. WT by Student's t-test.

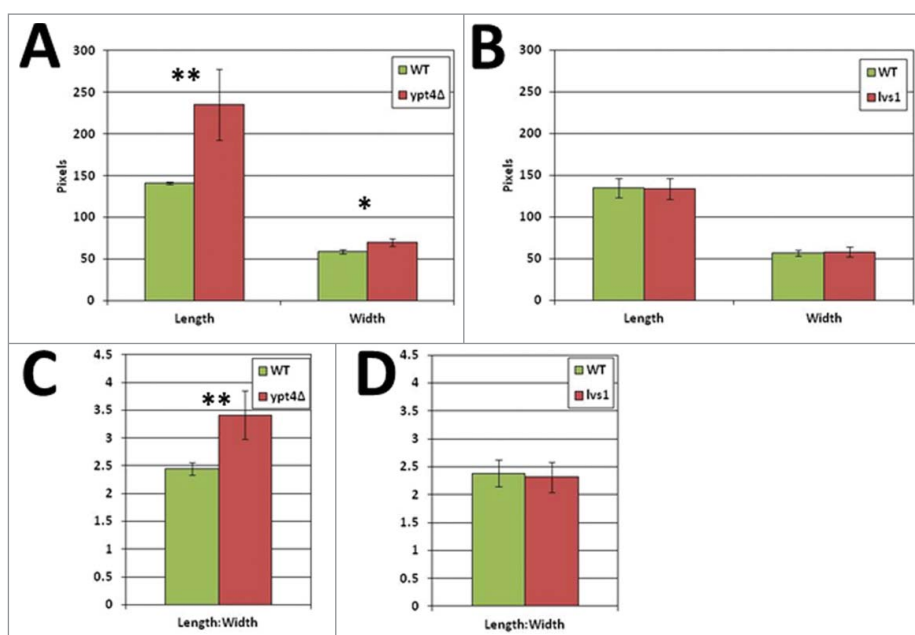


**Figure 2.** Deletion of *ypt4*, but not *lvs1*, results in an increase in cell size. Images of WT, *ypt4Δ*, and *lvs1Δ* cells were captured by differential interference microscopy. Cell length and width (in pixels) were measured using Image J. Length and width of (A) *ypt4Δ* or (B) *lvs1Δ* cells were measured (in pixels) using Image J and compared with that of the WT cells. The length:width ratio of (C) *ypt4Δ* or (D) *lvs1Δ* cells was also calculated and compared with that of the WT cells. Error bars represent the mean  $\pm$  SD. Significant differences were assessed using Student's *t*-test \* $p < 0.05$ ; \*\* $p < 0.02$ .

analyzed general endocytic and secretory trafficking pathways in cells lacking *ypt4* or *lvs1*. Endocytosis was quantitatively analyzed by monitoring FM4-64 uptake using flow cytometry. Inhibition of endocytosis using  $\text{NaN}_3$  and NaF has previously been shown to inhibit FM4-64 uptake.<sup>23</sup> Over 30 minutes, we observed no differences in FM4-64 uptake between WT, *ypt4Δ*, and *lvs1Δ* cells (Fig. 4A). Secretion of the enzyme cargo acid phosphatase was also similar between the three strains (Fig. 4B). Brefeldin A (BFA) is a fungal metabolite that has been shown to inhibit protein secretion in many organisms, including fission yeast.<sup>29</sup> Consistent with the absence of defects in secretion of acid phosphatase, neither *ypt4Δ* or *lvs1Δ* cells exhibited sensitivity to BFA (Fig. 4C). These results suggest that changes in vacuolar size in *ypt4Δ* and *lvs1Δ* cells are not due to general alterations in membrane trafficking pathways.

In CHS, defective biogenesis of lysosomes and lysosome-related organelles has been shown to result in impaired function,<sup>7</sup> and fission yeast strains with impaired vacuolar biogenesis or acidification have been shown to be sensitive to  $\text{CaCl}_2$  (*vps33Δ*, *vma1Δ*, *vma3Δ*) and/or neutral pH (*vma1Δ*, *vma3Δ*).<sup>30,31</sup> Therefore, to test whether vacuolar function was impaired in the *ypt4Δ* and *lvs1Δ* strains, we assessed growth on neutral (pH 7) media and media containing 50 mM  $\text{CaCl}_2$ . Both the *ypt4Δ* and *lvs1Δ* strains were sensitive to neutral pH and  $\text{CaCl}_2$  (Fig. 4D). These results suggest that vacuolar function is impaired by loss of *ypt4* or *lvs1*.

## Discussion

Our results demonstrate that both *ypt4p* and *lvs1p* play key roles in maintaining vacuolar function and homeostasis in fission yeast. These findings also establish fission yeast as a model for Chediak-Higashi Syndrome by showing that fission yeast *lvs1* functions similarly to the mammalian *LYST*,<sup>32</sup> with *lvs1*

deletion resulting in enlarged vacuoles. In contrast to these observations in fission yeast, deletion of the budding yeast *LYST* homolog *bph1* did not affect vacuolar morphology, although vacuolar protein sorting was mildly impaired.<sup>14</sup> These data establish key differences between budding yeast and fission yeast with respect to vacuolar biogenesis pathways. These distinct pathways may contribute to the differences in vacuole morphology between the 2 organisms.

Several mechanisms have been suggested to contribute to the development of enlarged lysosomes and LROs in CHS. *LYST* and its homologs in other organisms have been proposed to serve as positive regulators of lysosomal fission,<sup>9</sup> negative regulators of lysosomal fusion,<sup>10</sup> and/or positive regulators of biogenesis of post-lysosomes and fusion of these organelles (and other LROs) with the cell surface.<sup>11-13</sup> Although our results do not differentiate between these possibilities, we do show that overexpression of *lvs1*-YFP resulted in the presence of smaller vacuoles, suggesting that a role in vacuolar fission or fusion in yeast is likely. Based on observations in higher eukaryotes mentioned in the third mechanism above,<sup>11-13</sup> it will be interesting to explore a potential role in post-vacuolar sorting in fission yeast in future studies. To our knowledge, no evidence of post-vacuolar traffic has been shown in yeast, although it has been proposed as a potential pathway.<sup>1</sup>

Although our results do not define the downstream mechanisms regulated by *lvs1*, they do suggest that *ypt4* may act upstream of *lvs1* in control of lysosomal homeostasis. In mammalian cells, Rab4 isoforms have primarily been implicated in endosomal traffic.<sup>33,34</sup> However, a recent report shows that inhibition of endosomal sorting by expression of a dominant-negative Rab4 allele affects lysosomal biogenesis in *Drosophila*.<sup>35</sup> Furthermore, proper endosomal biogenesis has been implicated in development of secretory lysosomes in CHS.<sup>13</sup> Thus, the role of *ypt4* in maintenance of vacuolar homeostasis

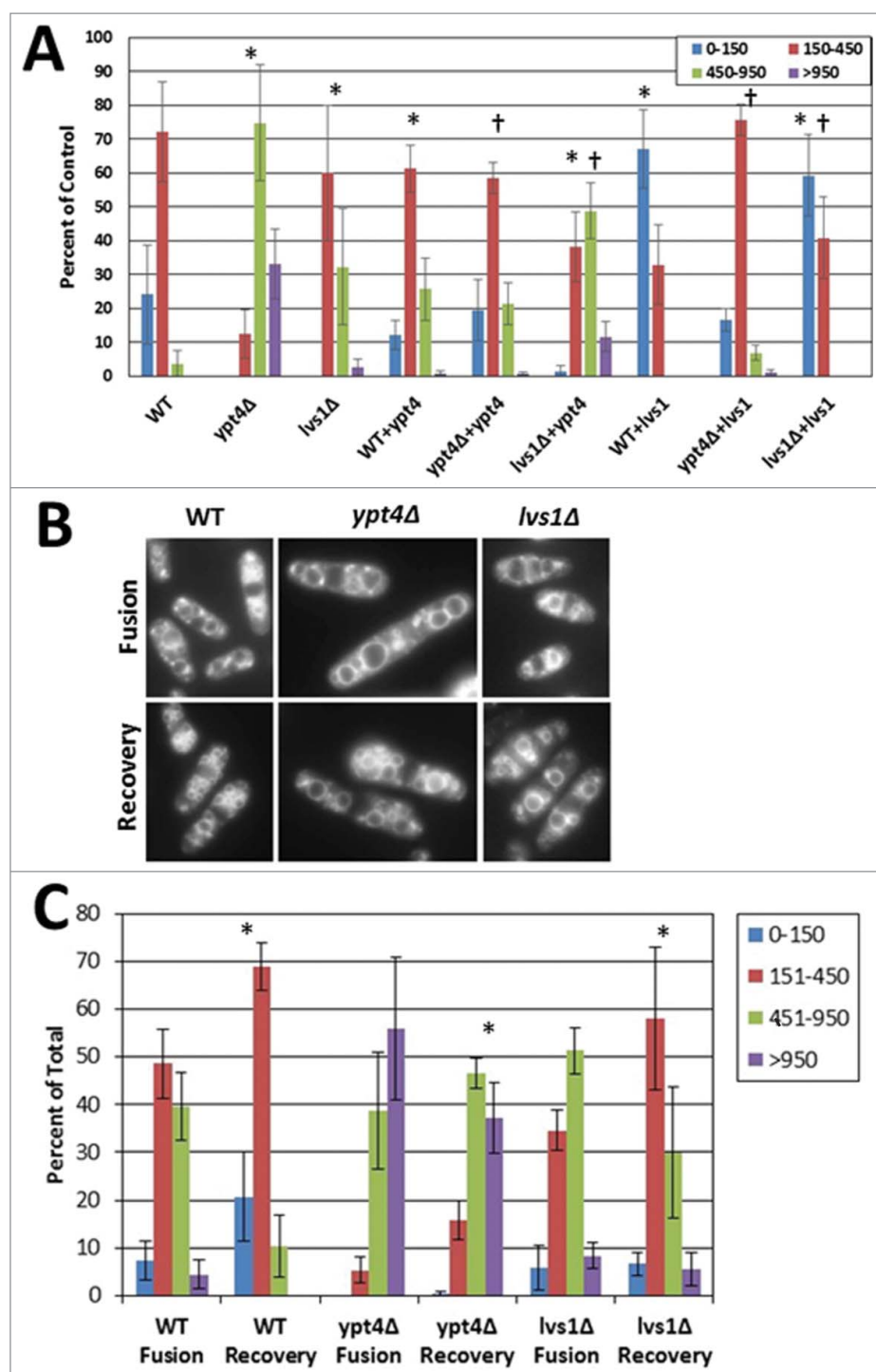


**Figure 3.** Lvs1p acts downstream of ypt4p to drive vacuolar fission. (A) WT, *ypt4Δ*, and *lvs1Δ* control cells and cells overexpressing Lvs1-YFP or ypt4-YFP were stained with FM4-64 for 20 min at 30°C, followed by washing and incubation at 30°C for an additional 30 minutes. The pixel area of the largest vacuole in each cell was measured using ImageJ software. For overexpression strains, only cells with visible YFP expression were scored. The percentage of cells containing vacuoles of the indicated pixel areas were calculated for each strain. Data are presented as the mean  $\pm$  SEM. Significant differences assessed by one-way ANOVA followed by post-hoc Student's t-test using Bonferroni's correction: \*  $P < 0.001$  vs. WT, † vs. the parent strain (*lvs1Δ* or *ypt4Δ*). (B) WT, *ypt4Δ*, and *lvs1Δ* cells were stained with FM4-64 for 20 min at 30°C, followed by incubation in dH<sub>2</sub>O for 90 minutes at 30°C (fusion). After washing, cells were allowed to recover for 90 minutes in media at 30°C (recovery). Cells were imaged by fluorescence microscopy. (C) Quantification of (A) The pixel area of the largest vacuole in each cell was measured using ImageJ software. The percentage of cells containing vacuoles of the indicated pixel areas were calculated for each strain. Data are presented as the mean  $\pm$  SEM. Significant differences assessed by ANOVA followed by post-hoc Student's t-test using Bonferroni's correction: \*  $P < 0.001$  vs. fusion in the same strain.

in fission yeast may be conserved in higher eukaryotes. However, the interpretation of these results is complicated by the lack of membrane targeting of overexpressed ypt4-YFP, potentially implicating ypt4-YFP in a signaling role that contributes to vacuolar homeostasis, rather than a trafficking role.

The precise mechanistic connection between ypt4p and lvs1p remains unclear. A previous study has shown that activation of the sty1 MAPK pathway can drive vacuolar fission in *ypt4Δ* cells.<sup>17</sup> This raises the question of whether lvs1p may be a direct or indirect target of the sty1 MAPK pathway. Bioinformatic



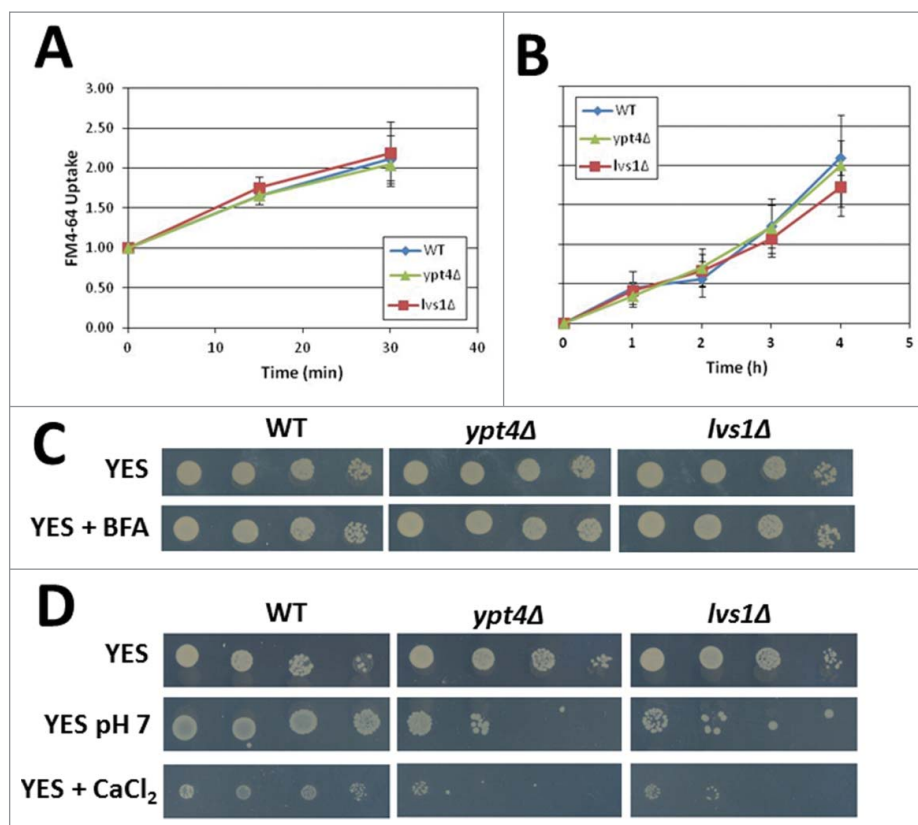


**Figure 4.** Deletion of *ypt4* or *lvs1* affects vacuolar function. (A) WT, *lvs1Δ*, and *ypt4Δ* cells were incubated with 32  $\mu$ M FM4–64 for the indicated times at 30°C, followed by extensive washing. FM4–64 uptake was measured by flow cytometry. Mean fluorescence was normalized to the 0 min timepoint for each strain. (B) Equal numbers of WT, *lvs1Δ*, and *ypt4Δ* cells were used to inoculate YES media. At the indicated times, an aliquot of the media was subjected to spectrophotometric determination of acid phosphatase activity by incubation with 2 mM p-nitrophenyl phosphate for 5 min, followed by measurement of the optical density of the sample at 405 nm. OD<sub>405</sub> values were normalized to the 0 h timepoint for each strain. Results are reported as mean  $\pm$  SEM for (A) and (B). C, D. Cells were subjected to a 10-fold serial dilution and were spotted on YES or YES + 10  $\mu$ g/mL BFA (C) or YES; YES + 10 mM Tris-HCl, pH 7; or YES + 50 mM CaCl<sub>2</sub> (D). Plates were incubated for 3–4 d at 30°C.

analysis suggests that *lvs1p* possesses three potential *styl1* phosphorylation sites (S147, S1157, and T1210).<sup>36,37</sup> Furthermore, in *Arabidopsis*, Lyst-interacting protein 5 (Lip5) is phosphorylated by the MAP kinases MPK3/6 to regulate multivesicular body biogenesis in the plant's defense against pathogens.<sup>38</sup> Thus, *lvs1p* and/or its regulators may be downstream target(s) of the stress-responsive *styl1* MAPK pathway. Interestingly, in mammalian cells, the p38 pathway (analogous to *styl1*) is also activated in response to stress<sup>39</sup> and has been implicated in regulation of lysosomal biogenesis,<sup>40</sup> as well as some types of autophagy.<sup>41,42</sup> These observations suggest the potential for a conserved eukaryotic pathway that regulates lysosomal/vacuolar homeostasis in response to environmental stress and suggest a new avenue of exploration to better understand the regulation and function of mammalian LYST proteins.

Another interesting phenotype noted in this report is the increase in length and width of *ypt4Δ* cells. This fairly uncommon phenotype has also been observed in the *tor1-L2045D* mutant at the restrictive temperature,<sup>22</sup> in *tor1* and *ssp1* mutants in response to low glucose, and in yeast overproducing the *ppe1p* or *ppa2p* phosphatases.<sup>2</sup> These results suggest that *ypt4p* may play a role in a signaling pathway that coordinates cell growth and cell division in response to nutrient availability. Consistent with this idea, the highly enlarged vacuoles observed in *ypt4Δ* cells are reminiscent of those observed in fission yeast cells subjected to glucose deprivation,<sup>43</sup> and glucose deprivation also

regulates TORC2 activity.<sup>44</sup> Furthermore, *TOR1* has been shown to regulate a vacuole inheritance cell cycle checkpoint in *S. cerevisiae*,<sup>45</sup> and the vacuole has been suggested to scale with cell size in budding yeast.<sup>46</sup> These observations suggest that *ypt4p* may connect a vacuole-dependent, nutrient sensing and scaling mechanism to control of the cell cycle. Thus, the increased size of *ypt4Δ* mutant cells may result from uncoupling of cell division from control of cell size and nutrient availability.

This potential role for *ypt4* and its homologs may be conserved in higher eukaryotes. The human Rab4 protein has been shown to undergo reversible phosphorylation at a consensus site for Cdk1/p34cdc2 kinase to regulate its membrane association during entry into mitosis.<sup>47</sup> Importantly, Cdk1/p34cdc2 has also been shown to phosphorylate Raptor, a key regulator of mTOR activity, suggesting that Rab4 and mTOR may be coordinately regulated at the G2/M transition in mammalian cells.<sup>48</sup> Thus, *rab4* may also play an important role in mTOR-dependent cell cycle transitions in mammalian cells, although this hypothesis requires further investigation.

Together, these observations suggest interesting new directions to explore in both yeast and mammalian systems. Are LYST/*lvs1* MAPK substrates that are activated in response to cell stress? Are *ypt4p*/*Rab4A*/*Rab4B* master regulators that integrate lysosomal/vacuolar function and nutrient sensing with cell cycle progression? These are interesting questions that could lead to novel directions to better understand Chediak-Higashi

Syndrome, as well as the general role of the lysosome and vacuole as a stress-responsive organelle in eukaryotes.

## Materials and methods

### Strains, yeast culture, and DNA manipulations

Strains used in this study are listed in Table 1. All strains were purchased from Bioneer (Alameda, CA). Cells were cultured at 30°C in Yeast Extract plus Supplements (YES; Sunrise Science Products; San Diego, CA) or Edinburgh Minimal Media (EMM; Sunrise Science Products) containing appropriate nutritional supplements. Deletion mutants were selected by growth on YES media containing 200 µg/mL G418.

pDUAL-YFH1c vectors carrying *ypt4*-YFP (SPAC1B3.11c) and *lvs1*-YFP (SPBC28E12.06c) under control of the full-strength *nmt1+* promoter were purchased from the Riken Bioresource Center DNA Bank (Ibaraki, Japan, deposited by M. Yoshida<sup>49–51</sup>). Plasmids were transformed into the WT, *ypt4*Δ, and *lvs1*Δ strains by the lithium acetate method, as described previously.<sup>52</sup> Transformants were selected on EMM containing appropriate supplements.

### MDY-64 staining and fluorescence microscopy

Wildtype (WT), *lvs1*Δ, and *ypt4*Δ cultures were resuspended in HEPES/glucose buffer (10 mM HEPES, pH 7.4; 5% glucose) containing 10 µM MDY-64 (ThermoFisher Scientific; Waltham, MA). After incubating 3 minutes at room temperature, the cells were washed in HEPES/glucose buffer. Vacuoles were imaged using a Zeiss Axioskop 2 fluorescence microscope (Zeiss; Oberkochen, Germany). Experiments were repeated a minimum of 3 times using independent cultures, and 10–15 images were captured per sample. Image J was used to quantify vacuole size as described previously.<sup>27</sup> Results are reported as the mean ± standard error of the mean (SEM).

### Quantification of cell size

To quantify cell size, images of the indicated cells were captured on the Zeiss Axioskop 2 described above using a differential interference contrast (DIC) filter. Cell length and width were measured in pixels using Image J. Results are reported as the mean ± standard deviation (SD) of 3 independent experiments.

### FM4-64 staining, vacuolar fusion, and endocytosis assays

FM4-64 staining was performed as described previously.<sup>17,27</sup> Briefly, cultures (WT, *ypt4*Δ, *lvs1*Δ, and *ypt4*-YFP and *lvs1*-YFP overexpression, as indicated) were resuspended in fresh YES media containing 32 µM FM4-64 (ThermoFisher Scientific) and incubated at 30°C for 20 minutes. After washing, the

cells were resuspended in fresh YES media and incubated at 30°C for 30 min to facilitate delivery of FM4-64 to the vacuole. After washing, cells were imaged as described above.

For vacuolar fusion and recovery assays, WT, *ypt4*Δ, and *lvs1*Δ cells were stained with FM4-64, as described above. To induce fusion, instead of resuspending cells in fresh YES media, cells were resuspended in dH<sub>2</sub>O and incubated for 90 min,<sup>17,27</sup> followed by washing. Cells that underwent recovery were incubated for an additional 90 min at 30°C before imaging and vacuolar quantification as described above.

For quantification of FM4-64 endocytosis, WT, *ypt4*Δ, and *lvs1*Δ cultures were resuspended in fresh YES media containing 32 µM FM4-64 (ThermoFisher Scientific; Waltham, MA) and incubated at 30°C for 0, 15, or 30 minutes. Cells were then washed 3 times with ice-cold YES media. FM4-64 fluorescence per cell was measured using a BD Accuri C6 Flow Cytometer (BD Biosciences; San Jose, CA). Mean fluorescence intensities were calculated for samples of at least 10,000 cells. Results represent the mean ± SEM from 3 independent experiments.

### Acid phosphatase secretion

Secretion of acid phosphatase activity was assayed as described previously.<sup>27,28</sup> Equal numbers of WT, *ypt4*Δ, and *lvs1*Δ cells were resuspended in fresh YES media and incubated at 30°C for the indicated times. At each timepoint, a media sample was collected for acid phosphatase secretion analysis and immediately subjected to centrifugation at 25000 × *g* for 1 min. Supernatants were stored at 4°C until all samples were collected. Acid phosphatase activity was assayed by incubating each sample with an equal volume of substrate solution (2 mM *p*-nitrophenyl phosphate, 0.1 M sodium acetate, pH 4.0) for 5 min at 30°C. The reaction was stopped by the addition of 0.33 M NaOH. Phosphatase activity was quantified by measuring the absorbance of each reaction at 405 nm (OD<sub>405</sub>). Results represent the mean ± SEM from 3 independent experiments.

### Spot assays

Equal numbers of WT, *lvs1*Δ, and *ypt4*Δ cells were subjected to a 10-fold serial dilution, and 5 µL of the resulting dilutions were spotted on the following plates: YES; YES + 10 µg/mL Brefeldin A (BFA); YES + 10 mM Tris-HCl, pH 7; and YES + 50 mM CaCl<sub>2</sub>. The plates were incubated at 30°C for 3–4 d before imaging.

### Statistical analyses

Statistical analyses were performed on a minimum of 3 independent experiments, comprising a minimum of 60 cells per strain. Significant differences between paired samples were analyzed using Student's *t*-test, and *p*-values less than 0.05 were deemed statistically significant. For multiple comparisons, or one-way analysis of variance (ANOVA) was used, followed by post-hoc Student's *t*-test using Bonferroni's correction.

**Table 1.** *S. pombe* strains used in this study.

Strain	Genotype	Source
Wildtype (WT)	<i>ade6</i> -M210 <i>ura4</i> -D18 <i>leu1</i> -32 <i>h</i> <sup>+</sup>	Bioneer
<i>ypt4</i> Δ	<i>ypt4</i> Δ:: <i>kanMX4</i> <i>ade6</i> -M210 <i>ura4</i> -D18 <i>leu1</i> -32 <i>h</i> <sup>+</sup>	Bioneer
<i>lvs1</i> Δ	<i>lvs1</i> Δ:: <i>kanMX4</i> <i>ade6</i> -M210 <i>ura4</i> -D18 <i>leu1</i> -32 <i>h</i> <sup>+</sup>	Bioneer

## Bioinformatic analyses

Identification of putative sty1p phosphorylation sites in lvs1p was performed using NetPhosYeast 1.0<sup>36</sup> and NetPhos 3.1.<sup>37</sup> Putative sty1p phosphorylation sites were defined as residues predicted to be phosphorylated in yeast using NetPhosYeast and predicted to be p38 consensus sites using NetPhos 3.1.

## Disclosure of potential conflicts of interest

No potential conflicts of interest were disclosed.

## Funding

This work was supported by NSF RUI MCB-1329506 and NSF MRI DBI-1229016.

## ORCID

Melanie L. Styers  <http://orcid.org/0000-0002-8234-6704>

## References

- Li SC, Kane PM. The yeast lysosome-like vacuole: endpoint and crossroads. *Biochim Biophys Acta* 2009; 1793(4):650-63; PMID:18786576; <https://doi.org/10.1016/j.bbamcr.2008.08.003>
- Yanagida M, Ikai N, Shimanuki M, Sajiki K. Nutrient limitations alter cell division control and chromosome segregation through growth-related kinases and phosphatases. *Philos Trans R Soc Lond B Biol Sci* 2011; 366(1584):3508-20; PMID:22084378; <https://doi.org/10.1098/rstb.2011.0124>
- Takegawa K, Iwaki T, Fujita Y, Morita T, Hosomi A, Tanaka N. Vesicle-mediated protein transport pathways to the vacuole in *Schizosaccharomyces pombe*. *Cell Struct Funct* 2003; 28(5):399-417; PMID:14745133; <https://doi.org/10.1247/csf.28.399>
- Huizing M, Boissy RE, Gahl WA. Hermansky-Pudlak syndrome: vesicle formation from yeast to man. *Pigment Cell Res* 2002; 15(6):405-19; PMID:12453182; <https://doi.org/10.1034/j.1600-0749.2002.02074.x>
- Huizing M, Anikster Y, Gahl WA. Hermansky-Pudlak syndrome and related disorders of organelle formation. *Traffic* 2000; 1(11):823-35; PMID:11208073; <https://doi.org/10.1034/j.1600-0854.2000.011103.x>
- Kaplan J, De Domenico I, Ward DM. Chediak-Higashi syndrome. *Curr Opin Hematol* 2008; 15(1):22-9; PMID:18043242; <https://doi.org/10.1097/MOH.0b013e3282f2bccc>
- Introne W, Boissy RE, Gahl WA. Clinical, molecular, and cell biological aspects of Chediak-Higashi syndrome. *Mol Genet Metab* 1999; 68(2):283-303; PMID:10527680; <https://doi.org/10.1006/mgme.1999.2927>
- Nagle DL, Karim MA, Woolf EA, Holmgren L, Bork P, Misumi DJ, McGrail SH, Dussault BJ Jr, Perou CM, Boissy RE, et al. Identification and mutation analysis of the complete gene for Chediak-Higashi syndrome. *Nat Genet* 1996; 14(3):307-11; PMID:8896560; <https://doi.org/10.1038/ng1196-307>
- Durchfort N, Verhoef S, Vaughn MB, Shrestha R, Adam D, Kaplan J, Ward DM. The Enlarged Lysosomes in beige(j) Cells Result From Decreased Lysosome Fission and Not Increased Lysosome Fusion. *Traffic* 2012; 13(1):108-19; PMID:21985295; <https://doi.org/10.1111/j.1600-0854.2011.01300.x>
- Kypri E, Falkenstein K, De Lozanne A. Antagonistic control of lysosomal fusion by Rab14 and the Lyst-related protein LvsB. *Traffic* 2013; 14(5):599-609; PMID:23387437; <https://doi.org/10.1111/tra.12058>
- Charette SJ, Cosson P. A LYST/beige homolog is involved in biogenesis of Dictyostelium secretory lysosomes. *J Cell Sci* 2007; 120(Pt 14):2338-43; PMID:17606989; <https://doi.org/10.1242/jcs.009001>
- Baetz K, Isaaq S, Griffiths GM. Loss of cytotoxic T lymphocyte function in Chediak-Higashi syndrome arises from a secretory defect that prevents lytic granule exocytosis. *J Immunol* 1995; 154(11):6122-31; PMID:7751653
- Sepulveda FE, Burgess A, Heiligenstein X, Goudin N, Menager MM, Romao M, Côte M, Mahlaoui N, Fischer A, Raposo G, et al. LYST controls the biogenesis of the endosomal compartment required for secretory lysosome function. *Traffic* 2015; 16(2):191-203; PMID:25425525; <https://doi.org/10.1111/tra.12244>
- Shiflett SL, Vaughn MB, Huynh D, Kaplan J, Ward DM. Bph1p, the *Saccharomyces cerevisiae* homologue of CHS1/beige, functions in cell wall formation and protein sorting. *Traffic* 2004; 5(9):700-10; PMID:15296494; <https://doi.org/10.1111/j.1600-0854.2004.00213.x>
- Notredame C, Higgins DG, Heringa J. T-Coffee: A novel method for fast and accurate multiple sequence alignment. *J Mol Biol* 2000; 302(1):205-17; PMID:10964570; <https://doi.org/10.1006/jmbi.2000.4042>
- Gaits F, Russell P. Vacuole fusion regulated by protein phosphatase 2C in fission yeast. *Mol Biol Cell* 1999; 10(8):2647-54; PMID:10436019; <https://doi.org/10.1091/mbc.10.8.2647>
- Bone N, Millar JB, Toda T, Armstrong J. Regulated vacuole fusion and fission in *Schizosaccharomyces pombe*: an osmotic response dependent on MAP kinases. *Curr Biol* 1998; 8(3):135-44; PMID:9443913; [https://doi.org/10.1016/S0960-9822\(98\)00060-8](https://doi.org/10.1016/S0960-9822(98)00060-8)
- Li SC, Diakov TT, Rizzo JM, Kane PM. Vacuolar H<sup>+</sup>-ATPase works in parallel with the HOG pathway to adapt *Saccharomyces cerevisiae* cells to osmotic stress. *Eukaryotic Cell* 2012; 11(3):282-91; PMID:22210831; <https://doi.org/10.1128/EC.05198-11>
- Cabrera M, Ostrowicz CW, Mari M, LaGrassa TJ, Reggiori F, Ungermann C. Vps41 phosphorylation and the Rab Ypt7 control the targeting of the HOPS complex to endosome-vacuole fusion sites. *Mol Biol Cell* 2009; 20(7):1937-48; PMID:19193765; <https://doi.org/10.1091/mbc.E08-09-0943>
- Kashiwazaki J, Iwaki T, Takegawa K, Shimoda C, Nakamura T. Two fission yeast rab7 homologs, ypt7 and ypt71, play antagonistic roles in the regulation of vacuolar morphology. *Traffic* 2009; 10(7):912-24; PMID:19453973; <https://doi.org/10.1111/j.1600-0854.2009.00907.x>
- Fratti RA, Jun Y, Merz AJ, Margolis N, Wickner W. Interdependent assembly of specific regulatory lipids and membrane fusion proteins into the vertex ring domain of docked vacuoles. *J Cell Biol* 2004; 167(6):1087-98; PMID:15611334; <https://doi.org/10.1083/jcb.200409068>
- Ikai N, Nakazawa N, Hayashi T, Yanagida M. The reverse, but coordinated, roles of Tor2 (TORC1) and Tor1 (TORC2) kinases for growth, cell cycle and separate-mediated mitosis in *Schizosaccharomyces pombe*. *Open Biol* 2011; 1(3):110007; PMID:22645648; <https://doi.org/10.1098/rsob.110007>
- Vida TA, Emr SD. A new vital stain for visualizing vacuolar membrane dynamics and endocytosis in yeast. *J Cell Biol* 1995; 128(5):779-92; PMID:7533169; <https://doi.org/10.1083/jcb.128.5.779>
- Farnsworth CC, Seabra MC, Ericsson LH, Gelb MH, Glomset JA. Rab geranylgeranyl transferase catalyzes the geranylgeranylation of adjacent cysteines in the small GTPases Rab1A, Rab3A, and Rab5A. *Proc Natl Acad Sci U S A* 1994; 91(25):11963-7; PMID:7991565; <https://doi.org/10.1073/pnas.91.25.11963>
- Gomes AQ, Ali BR, Ramalho JS, Godfrey RF, Barral DC, Hume AN, Seabra MC. Membrane targeting of Rab GTPases is influenced by the prenylation motif. *Mol Biol Cell* 2003; 14(5):1882-99; PMID:12802062; <https://doi.org/10.1091/mbc.E02-10-0639>
- Sonnichsen B, De Renzis S, Nielsen E, Rietdorf J, Zerial M. Distinct membrane domains on endosomes in the recycling pathway visualized by multicolor imaging of Rab4, Rab5, and Rab11. *J Cell Biol* 2000; 149(4):901-14; PMID:10811830; <https://doi.org/10.1083/jcb.149.4.901>
- Eckler AM, Wilder C, Castanon A, Ferris VM, Lamere RA, Perrin BA, Pearlman R, White B, Byrd C, Ludvik N, et al. Haploinsufficiency of the sec 7 guanine nucleotide exchange factor *gea1* impairs septation in fission yeast. *PLoS one* 2013; 8(2):e56807; <https://doi.org/10.1371/journal.pone.0056807>
- Kita A, Sugiura R, Shoji H, He Y, Deng L, Lu Y, Sio SO, Takegawa K, Sakaue M, Shuntoh H, et al. Loss of Apm1, the micro1 subunit of the clathrin-associated adaptor-protein-1 complex, causes distinct phenotypes and synthetic lethality with calcineurin deletion in fission yeast. *Mol Biol Cell* 2004; 15(6):2920-31; PMID:15047861; <https://doi.org/10.1091/mbc.E03-09-0659>

- [29] Turi TG, Webster P, Rose JK, Brefeldin A sensitivity and resistance in *Schizosaccharomyces pombe*. Isolation of multiple genes conferring resistance. *J Biol Chem* 1994; 269(39):24229-36; PMID:7929079
- [30] Iwaki T, Osawa F, Onishi M, Koga T, Fujita Y, Hosomi A, Tanaka N, Fukui Y, Takegawa K. Characterization of vps33+, a gene required for vacuolar biogenesis and protein sorting in *Schizosaccharomyces pombe*. *Yeast* 2003; 20(10):845-55; PMID:12868054; <https://doi.org/10.1002/yea.1011>
- [31] Iwaki T, Hosomi A, Tokudomi S, Kusunoki Y, Fujita Y, Giga-Hama Y, Tanaka N, Takegawa K. Vacuolar protein sorting receptor in *Schizosaccharomyces pombe*. *Microbiology* 2006; 152(Pt 5):1523-32; PMID:16622069; <https://doi.org/10.1099/mic.0.28627-0>
- [32] Barbosa MD, Nguyen QA, Tchernev VT, Ashley JA, Detter JC, Blydes SM, Brandt SJ, Chotai D, Hodgman C, Solari RC, et al. Identification of the homologous beige and Chediak-Higashi syndrome genes. *Nature* 1996; 382(6588):262-5; PMID:8717042; <https://doi.org/10.1038/382262a0>
- [33] van der Sluijs P, Hull M, Webster P, Male P, Goud B, Mellman I. The small GTP-binding protein rab4 controls an early sorting event on the endocytic pathway. *Cell* 1992; 70(5):729-40; PMID:1516131; [https://doi.org/10.1016/0092-8674\(92\)90307-X](https://doi.org/10.1016/0092-8674(92)90307-X)
- [34] Van Der Sluijs P, Hull M, Zahraoui A, Tavitian A, Goud B, Mellman I. The small GTP-binding protein rab4 is associated with early endosomes. *Proc Natl Acad Sci U S A* 1991; 88(14):6313-7; PMID:1906178; <https://doi.org/10.1073/pnas.88.14.6313>
- [35] Jacomin AC, Fauvarque MO, Taillebourg E. A functional endosomal pathway is necessary for lysosome biogenesis in *Drosophila*. *BMC Cell Biol* 2016; 17(1):36; PMID:27852225; <https://doi.org/10.1186/s12860-016-0115-7>
- [36] Ingrell CR, Miller ML, Jensen ON, Blom N. NetPhosYeast: prediction of protein phosphorylation sites in yeast. *Bioinformatics* 2007; 23(7):895-7; PMID:17282998; <https://doi.org/10.1093/bioinformatics/btm020>
- [37] Blom N, Sicheritz-Ponten T, Gupta R, Gammeltoft S, Brunak S. Prediction of post-translational glycosylation and phosphorylation of proteins from the amino acid sequence. *Proteomics* 2004; 4(6):1633-49; PMID:15174133; <https://doi.org/10.1002/pmic.200300771>
- [38] Wang F, Shang Y, Fan B, Yu JQ, Chen Z. Arabidopsis LIP5, a positive regulator of multivesicular body biogenesis, is a critical target of pathogen-responsive MAPK cascade in plant basal defense. *PLoS Pathog* 2014; 10(7):e1004243; PMID:25010425; <https://doi.org/10.1371/journal.ppat.1004243>
- [39] Mikhailov A, Shinohara M, Rieder CL. The p38-mediated stress-activated checkpoint. A rapid response system for delaying progression through antephase and entry into mitosis. *Cell Cycle* 2005; 4(1):57-62; PMID:15611649; <https://doi.org/10.4161/cc.4.1.1357>
- [40] Li Y, Xu M, Ding X, Yan C, Song Z, Chen L, Huang X, Wang X, Jian Y, Tang G, et al. Protein kinase C controls lysosome biogenesis independently of mTORC1. *Nature Cell Biol* 2016; 18(10):1065-77; PMID:27617930; <https://doi.org/10.1038/ncb3407>
- [41] Hirota Y, Yamashita S, Kurihara Y, Jin X, Aihara M, Saigusa T, Kang D, Kanki T. Mitophagy is primarily due to alternative autophagy and requires the MAPK1 and MAPK14 signaling pathways. *Autophagy* 2015; 11(2):332-43; PMID:25831013; <https://doi.org/10.1080/15548627.2015.1023047>
- [42] Hocker R, Walker A, Schmitz I. Inhibition of autophagy through MAPK14-mediated phosphorylation of ATG5. *Autophagy* 2013; 9(3):426-8; PMID:23235332; <https://doi.org/10.4161/auto.22924>
- [43] Pluskal T, Hayashi T, Saitoh S, Fujisawa A, Yanagida M. Specific biomarkers for stochastic division patterns and starvation-induced quiescence under limited glucose levels in fission yeast. *FEBS J* 2011; 278(8):1299-315; PMID:21306563; <https://doi.org/10.1111/j.1742-4658.2011.08050.x>
- [44] Hatano T, Morigasaki S, Tatebe H, Ikeda K, Shiozaki K. Fission yeast Ryh1 GTPase activates TOR Complex 2 in response to glucose. *Cell Cycle* 2015; 14(6):848-56; PMID:25590601; <https://doi.org/10.1080/15384101.2014.1000215>
- [45] Jin Y, Weisman LS. The vacuole/lysosome is required for cell-cycle progression. *eLife* 2015;4; PMID:26322385; <https://doi.org/10.7554/eLife.08160>
- [46] Chan YH, Marshall WF. Organelle size scaling of the budding yeast vacuole is tuned by membrane trafficking rates. *Biophys J* 2014; 106(9):1986-96; PMID:24806931; <https://doi.org/10.1016/j.bpj.2014.03.014>
- [47] van der Sluijs P, Hull M, Huber LA, Male P, Goud B, Mellman I. Reversible phosphorylation-dephosphorylation determines the localization of rab4 during the cell cycle. *EMBO J* 1992; 11(12):4379-89; PMID:1425574
- [48] Gwinn DM, Asara JM, Shaw RJ. Raptor is phosphorylated by cdc2 during mitosis. *PLoS One* 2010; 5(2):e9197; PMID:20169205; <https://doi.org/10.1371/journal.pone.0009197>
- [49] Matsuyama A, Shirai A, Yashiroda Y, Kamata A, Horinouchi S, Yoshida M. pDUAL, a multipurpose, multicopy vector capable of chromosomal integration in fission yeast. *Yeast* 2004; 21(15):1289-305; PMID:15546162; <https://doi.org/10.1002/yea.1181>
- [50] Matsuyama A, Yoshida M. Systematic cloning of an ORFeome using the Gateway system. *Methods Mol Biol* 2009; 577:11-24; PMID:19718505; [https://doi.org/10.1007/978-1-60761-232-2\\_2](https://doi.org/10.1007/978-1-60761-232-2_2)
- [51] Matsuyama A, Arai R, Yashiroda Y, Shirai A, Kamata A, Sekido S, Kobayashi Y, Hashimoto A, Hamamoto M, Hiraoka Y, et al. ORFeome cloning and global analysis of protein localization in the fission yeast *Schizosaccharomyces pombe*. *Nat Biotechnol* 2006;24(7):841-7; PMID:16823372; <https://doi.org/10.1038/nbt1222>
- [52] Bahler J, Wu JQ, Longtine MS, Shah NG, McKenzie A, 3rd, Steever AB, Wach A, Philippsen P, Pringle JR. Heterologous modules for efficient and versatile PCR-based gene targeting in *Schizosaccharomyces pombe*. *Yeast* 1998; 14(10):943-51; PMID:9717240; [https://doi.org/10.1002/\(SICI\)1097-0061\(199807\)14:10<943::AID-YEA292>3.0.CO;2-Y](https://doi.org/10.1002/(SICI)1097-0061(199807)14:10<943::AID-YEA292>3.0.CO;2-Y)